Methylene Blue Adsorption from Aqueous Solution Using $Zn_2(Bdc)_2(Dabco)$ Metal-Organic Framework and Its Polyurethane Nanocomposite

Motakef Kazemi*[*+], Negar

Department of Medical Nanotechnology, Faculty of Advanced Sciences and Technology, Tehran Medical Sciences, Islamic Azad University, Tehran, I.R. IRAN

Asadi, Atefeh

Department of Nanochemistry, Faculty of Pharmaceutical Chemistry, Tehran Medical Sciences, Islamic Azad University, Tehran, I.R. IRAN

ABSTRACT: *In this work, $Zn_2(BDC)_2(DABCO)$ Metal-Organic Framework (MOF) was prepared by Zn = zinc acetate dehydrates, BDC = 1,4-benzenedicarboxylate, and DABCO = 1,4-diazabicyclo [2.2.2] octane. The MOF and its polyurethane (PU) nanocomposite were used to remove Methylene Blue (MB) as a harmful and toxic dye from an aqueous solution. Polyurethane polymer has been modified with a zinc-based metal-organic framework by the press method to develop an efficient adsorbent for the first time. Samples were characterized by Fourier Transform InfraRed (FT-IR) spectroscopy to evaluate functional groups, X-Ray Diffraction (XRD) analysis of crystal structure, field emission scanning electron microscope (FESEM) to determine morphology and size, BET analysis for measurement of surface area, and Ultraviolet–Visible (UV–Vis) spectroscopy to study MB adsorption. Methylene blue adsorption was reported by changing the amount of adsorbent, MB concentration, pH, and temperature of the solution over time. According to the results, increasing the amount and percentage of adsorbent, pH, and temperature of the solution increased the percentage of adsorption efficiency. Also, the MOF and its nanocomposite can be a good choice for the adsorption of methylene blue as a cationic dye due to its high level and low material consumption. The results show that $Zn_2(BDC)_2(DABCO)$ MOF and its PU nanocomposite can have good potential for the development of various adsorbents.*

KEYWORDS: *Adsorption; Methylene blue; MOF; Nanocomposite; Polyurethane.*

INTRODUCTION

Toxic dyes are one of the main pollutants with harmful effects on the environment and living organisms [1]. Methylene blue is a toxic cationic dye in wastewaters of various industries such as textile, paper, leather, plastic, food processing, cosmetics, printing, pharmaceutical, and dye production [2]. Methylene blue is one of the most

* *To whom correspondence should be addressed.*
+E-mail address: motakef@iaups.ac.ir
1021-9986/2022/12/3950-3962 13/$/6.03

common cation dye members and is widely used in the textile industry for dyeing cotton and wool fabrics [3]. MB with the formula $[(CH_3)_2N(C_6H_3)NS^+(C_6H_3)N(CH_3)_2Cl^-]$, is one of the monovalent cationic dyes with S and N linkage [4]. The presence of MB dye in water reduces the transmission of sunlight, and reduces the natural photosynthetic activity and acute and chronic toxicity of ecosystems [5]. Methylene blue dye has several harmful effects including shortness of breath, nausea, vomiting, and gastritis. Therefore, various methods have been developed to remove organic dyes from an aqueous solution such as physical, chemical, and biological methods [6]. Among the various methods, adsorption technology is considered a competitive method of dye removal due to its high efficiency, economic feasibility, and design simplicity [7, 8]. The application of adsorbent is important for the absorption of pollutants from aqueous solutions under different conditions [9-14]. Today, the process of absorption from wastewater has been expanded due to the surface-active group [15-17]. In the last decade, dye adsorption has been a real challenge due to its widespread use worldwide [18-25]. Today, nanostructures have a good potential to absorb methylene blue dye due to their high surface area [26-28]. According to the results, the interaction between the adsorbent and the dye affects the efficiency of the adsorption process [29, 30]. The adsorption mechanisms are responsible for dye removal based on electrostatic attraction, ion exchange, surface complexity, and π-π interactions [31]. In general, there are many ways to improve physicochemical properties and adsorption performance in wastewater treatment technologies. That should be considered first, physical modification to improve the absorption behavior; second, stability in the environment; third, the loading of the target material inside the structure and the improvement of the surface area and absorption properties [32]. Nanocomposites consisting of two parts, organic and inorganic can play an effective role in improving adsorption [33]. Immobilization of the adsorbent on the solid support is also one of the ways to help the adsorption [34]. However, the main drawbacks of immobilization are the significant reduction in its efficiency due to the drastic reduction of the effective surface and their mass transfer, as well as the need to search for methods and equipment [35]. Therefore, the importance of this study is to investigate the adsorption of methylene blue cationic dye based on new materials and methods.

Metal-organic framework is a new class of coordination polymers [36]. These highly porous crystalline materials contain organic ligands as linkers and metal ions or clusters as metal centers [37, 38]. In recent years, MOFs have received much attention due to their unique properties for various applications [39, 40]. Metal-organic frameworks are typically synthesized by solution [41], solvothermal [42], hydrothermal [43], microwave [44], sonochemical [45], electrochemical [46], mechanochemical [47], and laser ablation methods [48, 49]. MOFs are a good candidate as dye adsorbent [50]. Recently, the metal-organic framework has been used as an efficient absorbent [51] and removal [52, 53] of an aqueous solution. These porous compounds have been expanded to adsorb methylene blue by copper-MOF [54], iron-MOF [55-58], nickel-MOF [59], zirconium-MOF [60], aluminum-MOF [61], and cobalt-MOF [62]. $Zn_2(BDC)_2(DABCO)$ is a good candidate MOF based on zinc metal (Zn-MOF) with various potential applications. This MOF is synthesized by self-assembly of Zn_4O units and 1,4-benzenedicarboxylate and 1,4-diazabicyclo [2.2.2] octane ligands [42, 43]. According to the functional groups in $Zn_2(BDC)_2(DABCO)$, MB dye adsorption is important in the present study and the MOF can be a good candidate for MB dye adsorption.

Recently, nanotechnology adsorption technologies have attracted the attention of the scientific community as a promising treatment method. Easy separation of water by polymeric [63] and iron oxide [62, 64] sorbents is a useful adsorbent advantage during treatment. Eco-friendly nanocomposites were investigated for cationic dye-treated wastewater [65]. Polymer-based adsorbents have been developed for efficient removal due to the simplicity of the preparation method [66]. Polymer nanocomposite can play an important role in expanding the dye removal goal [67]. Polyurethane is a common polymer with excellent mechanical properties and good water resistance for widespread use in different applications. Recently, polyurethane nanocomposites have been reported to adsorb dyes from aqueous solutions [68]. The aim of this study was to develop a simple method for the preparation of zinc-based MOF and its nanocomposite as an effective adsorbent in the adsorption of methylene blue dye. Due to the mentioned advantages such as a simple preparation method with lower cost, in this study $Zn_2(BDC)_2(DABCO)$ MOF was used as adsorbent due to the simultaneous presence of the organic part and the possibility of

modifying and the inorganic part and the possibility of creating a high surface area. Also, $Zn_2(BDC)_2(DABCO)$ MOF-PU nanocomposite was prepared by a pressing method due to the filling of the MOF pores with solvent and the impossibility of adsorption by the casting method. The novelty of the work, the MOF and its nanocomposite were first evaluated as methylene blue adsorbent from aqueous.

EXPERIMENTAL SECTION

Materials

All reagents with high purity and analytical grade were purchased from Merck (Darmstadt, Germany). Ultra-pure water was used for the preparation of all reagent solutions. Zinc acetate dehydrates ($Zn(Oac)_2.2H_2O$) salt, 1,4 benzenedicarboxylic acid ligand, 1,4-diazabicyclo [2.2.2] octane ligand, and dimethyl formamide (DMF) solvent were used for synthesis of the Zn-MOF. The tetrahydrofuran (THF) solvent was used to dissolve the PU polymer (with 1400 g/mol molecular weight, Apilon 52 DE 40). Methylene blue ($C_{16}H_{18}ClN_3S$) was used as the cationic dye.

Preparation of samples

The $Zn_2(BDC)_2(DABCO)$ MOF was prepared by a solvothermal method using adding Zn $(OAc)_2.2H_2O$ (0.132 g, 2 mmol) to the production of Zn^{2+} ions as a connector, BDC (0.1 g, 2 mmol) as a chelating ligand, and DABCO (0.035 g, 1 mmol) as a bridging ligand to 25 mL DMF as a solvent [42]. The precursors were sealed under reflux and stirred at 90 °C for 3 h. The MOF can be prepared at different times including 15 min [19], 3 h [48], 24 h [43], and 72 h [41] but the optimized time is 3 h [69]. Then, the reaction mixture was cooled to room temperature and filtered. The white crystals were washed with DMF to remove any metal and ligands that remained and dried in a vacuum for faster drying. DMF was removed from white crystals with a vacuum furnace at 150 °C for 5 h.

The casting method is not suitable for the preparation of $Zn_2(BDC)_2(DABCO)$ MOF-polyurethane nanocomposites, because the MOF pores are filled with solvent in this method, as a result, no porosity to absorb the MB. Therefore, these nanocomposites were prepared by press method with different percentages of the MOF for the first time in this work. First, PU polymer was placed in a template and then placed at a temperature of 230 °C to form a homogeneous film. Then the MOF sample was uniformly put on the film and 50 kN was pressed at 130 ° C. The application of temperature is due to the fact that the film surface is ready to absorb the MOF, and the application of pressure in a short period of 2 min is due to the placement of the MOF on the film surface. Finally, the sample was placed in a cold press machine to stabilize the MOF samples on the polymer. Based on MB adsorption, PU nanocomposites with 5 and 10 % of the MOF were shown better results and it was not possible to form a uniform nanocomposite with a higher percentage of the MOF.

Characterization techniques

FT-IR spectra were recorded on a Shimadzu 460 spectrometer in a KBr matrix in the range of 400–4000 cm^{-1}. The crystalline structure of the sample was investigated by X-ray diffraction utilizing Cu Kα X-ray radiation with a voltage of 40 kV and a current of 30 mA by X'pert pro diffractometer (X' Pert Pro model, Panalytical, Peru). A field emission scanning electron microscope was employed to observe morphology and size (Sigma VP model, Zeiss, Germany). The surface area was determined using nitrogen gas sorption by the MOF samples at 298 K and 0.88-atmosphere pressure (BElSORP Mini model, Microtrac Bel Corp, Japan). Methylene blue adsorption was evaluated by UV–Vis spectroscopy (Genesys 30 model, Thermo Scientific, America).

RESULTS AND DISCUSSIONS

FT-IR

FT-IR spectra of MOF are presented before and after methylene blue adsorption (Fig. 1). The IR bands of O–H stretching and N–H asymmetric stretching are characteristic at ~3300 cm^{-1} [70-74]. Due to the presence of the hydroxyl group in the composition, the vibrational states at this wavelength are assignable to the O–H broad absorption mode [71]. The peak at 3050-3150 cm^{-1} is assigned with aromatic sp^2 C-H stretch bands. The aliphatic C–H asymmetric stretching vibration is assigned at ~2958 cm^{-1} [70, 71]. The O–H. . .O valance stretching vibration band is reported at ~2600 cm^{-1}. The high-intensity peak of C=O stretching is assigned at ~1635 cm^{-1} for $Zn_2(BDC)_2(DABCO)$ MOF. The bands of aromatic C=C stretching are shown at ~1593 cm^{-1}. The vibration of O–H bending from the water molecules adsorbed on the surface resulted in the absorption band at 1635 cm^{-1} [75]. The high-intensity peak of C=O carboxylic group is specified at ~1390 cm^{-1}. The FT-IR result is according to the report of methylene blue removal by MOF adsorbent [53, 54]. The MB adsorption is qualitatively approved by FT-IR spectra.

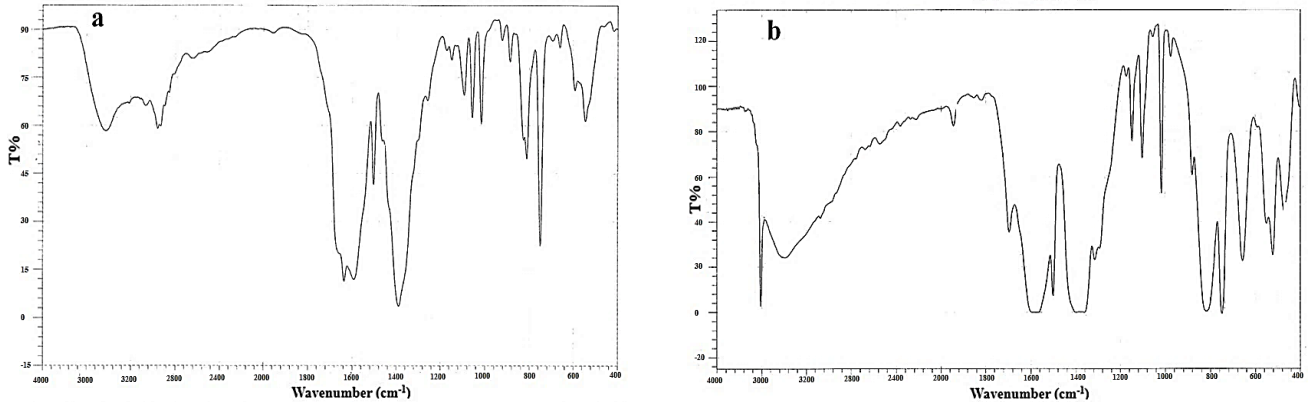

Fig. 1: FT-IR spectra of MOF a) before and b) after MB adsorption.

The peaks at ~1315 cm^{-1} and 817 cm^{-1} are assigned with the–CN (amide) vibration and $–CH_2$ (methylene) vibration, respectively which is reported in line with the results [73, 76]. After MB adsorption, new IR bands appear and many functional groups are undergone red or blue shifting [77]. These vibrations represent the interactions of methylene blue with functional groups of MOF adsorbent.

XRD

The XRD pattern of samples was measured in 2θ range 5-50° that used to identify the crystalline structure (Fig. 2). The XRD pattern of MOF is similar to a previously reported pattern and the crystalline structure is preserved after the adsorption based on the previous report [41, 42]. The XRD of polyurethane approved the crystalline structure according to the previous report with two characteristic peaks [75]. The high percentage of PU polymer in the nanocomposite caused no observation of MOF characteristic peaks and the result is according to the previous report [78]. The results confirmed that there has been a slight amount of material in the amorphous state [74].

FESEM

The FESEM images were shown for MOF before and after methylene blue adsorption and its nanocomposite (Fig. 3). SEM results were shown MOF nanostructures with rod morphology and diameter size of about 100 nm (before methylene blue adsorption) and about 90 nm (after methylene blue adsorption). As a result, homogenization has reduced the size for better MB adsorption. The FESEM of MOF-PU nanocomposite was shown in the form of an image from the cross-section. As a result, the presence of the MOF on PU polymer surface is confirmed. The result

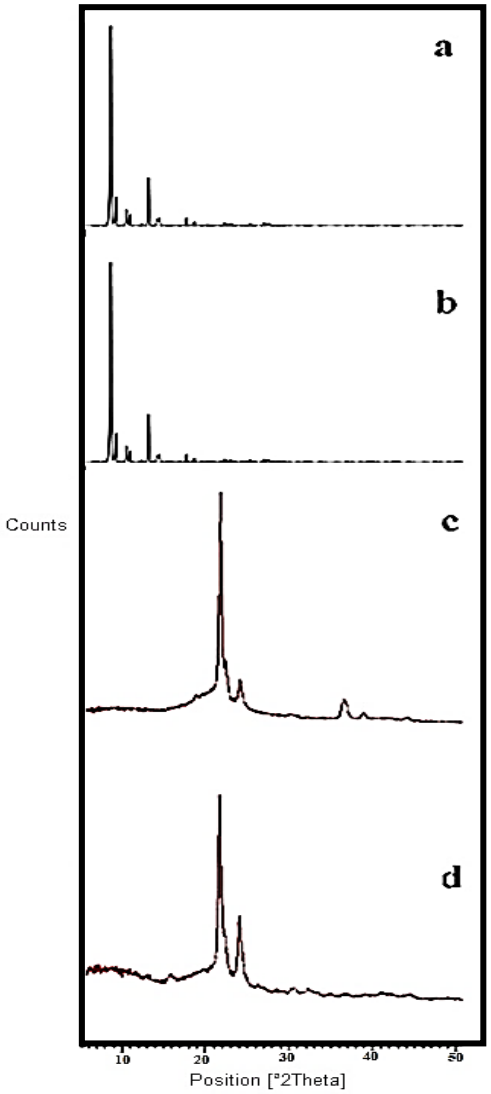

Fig. 2: XRD Pattern of a) MOF before MB adsorption, b) MOF after MB adsorption, c) PU polymer, and d) MOF-PU nanocomposite.

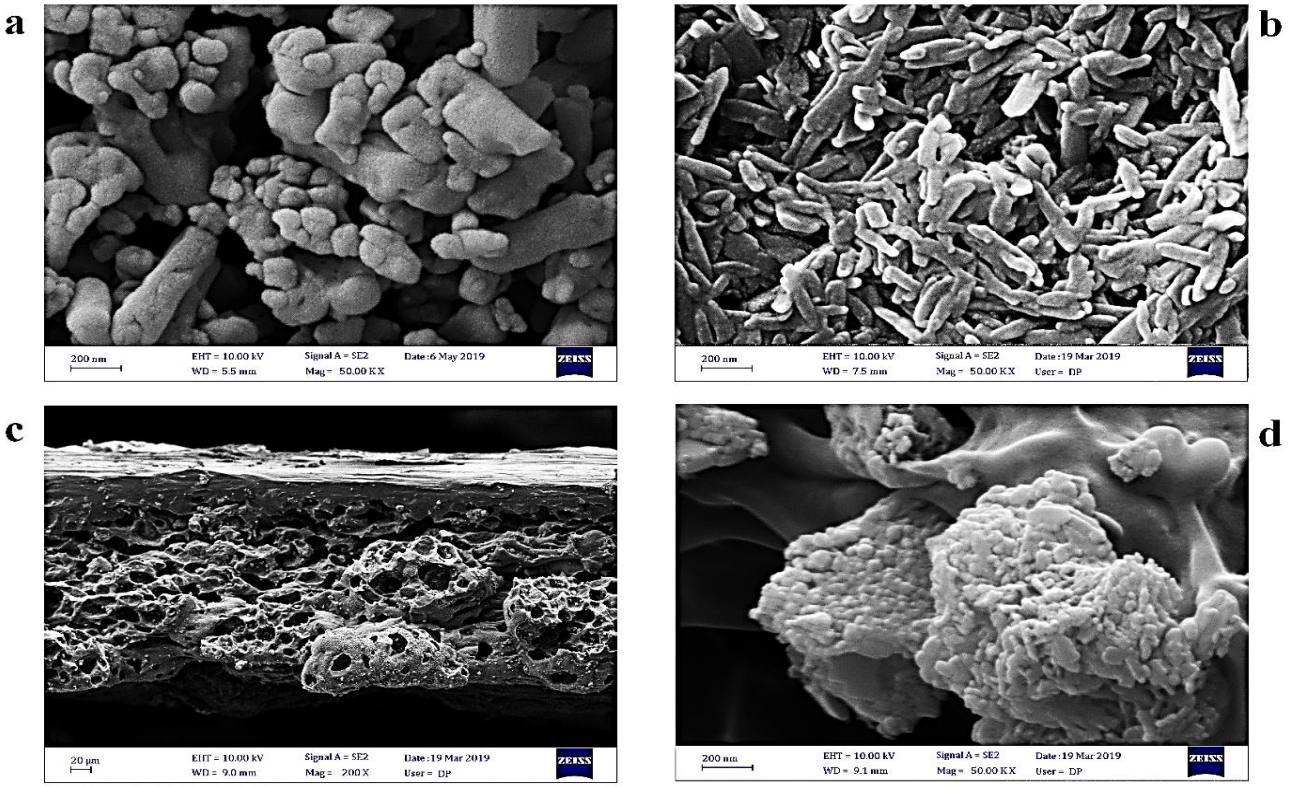

Fig. 3: FESEM images of a) MOF before MB adsorption, b) MOF after MB adsorption, cross-section image of MOF-PU nanocomposite c) in 20 µm scale bare, and d) in 200 nm scale bare.

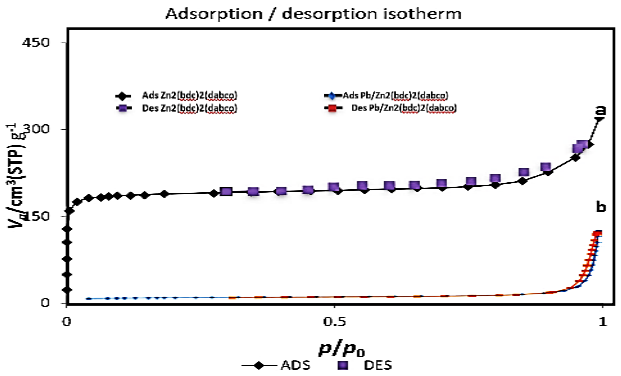

Fig. 4: The absorption/desorption N_2 curve related to MOF a) before and b) after MB adsorption.

is according to the previous report on copper adsorption by MOF-5 and its polyurethane nanocomposite [78].

BET

The Brunauer–Emmett–Teller (BET) analysis was used for the determination of the surface area of the MOF by N_2 adsorption before and after methylene blue adsorption (Fig. 4). The purpose of BET is to explain the physical adsorption of gas molecules on a solid surface as an analysis technique for measuring the specific surface area of materials. The surface area of the MOF was investigated by exiting the solvent at 150 °C for 5 h. Based on the results, it was found that type I Nitrogen isotherms (according to IUPAC classification) [79]. The surface area of MOF was decreased with methylene blue adsorption from 762 m^2/gr to 21 m^2/gr. The decrease in the surface area indicates that methylene blue is almost in almost all MOF pores after adsorption. The result is according to the previous report for methylene blue adsorption by Fe-type MOF [55].

UV–Vis spectroscopy

The methylene blue adsorption was investigated by UV–Vis spectroscopy. The calibration curve of methylene blue was examined at λ_{max} = 664 nm with a concentration of 0.5, 1, 2, 3, and 4 mg/L (Fig 5. a). The goal is to achieve high absorption even with small amounts to show capability adsorption capacity. The adsorption diagram was investigated by different MOF amounts including 0.125, 0.25, and 0.5 g for 2 mL methylene blue concentration at 4 mg/L at various times including 0.5, 1, 2, 3, and 4 h (Fig 5. b). The efficiency was calculated as follows:

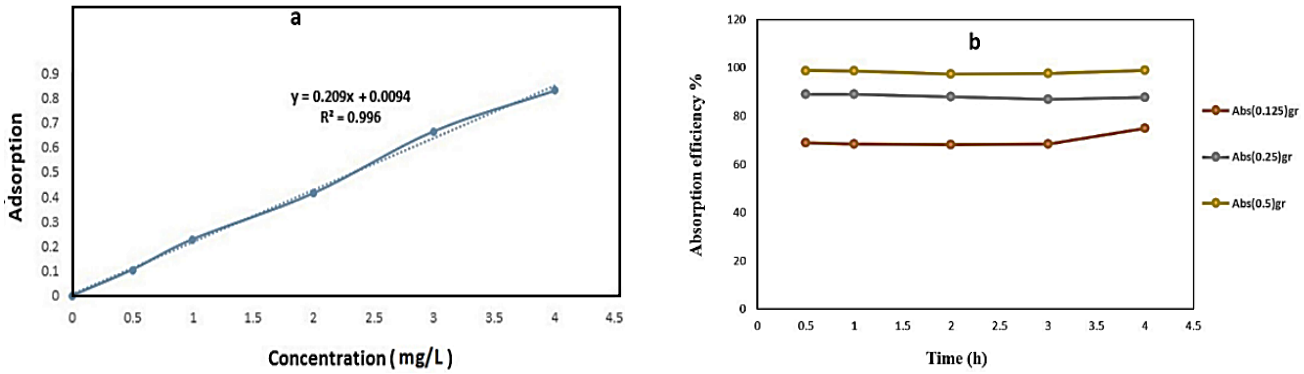

Fig. 5: a) The calibration curve of MB and b) the diagram of MB adsorption in different MOF amounts.

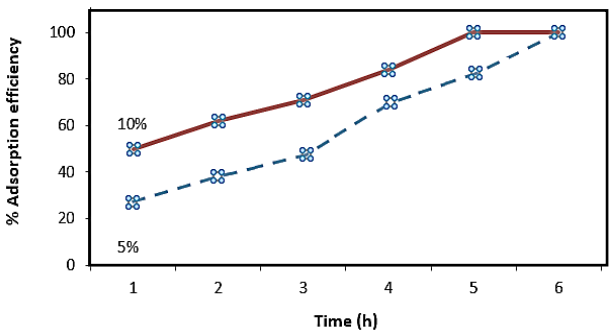

Fig. 6: The diagram of MB adsorption by a) MOF and b) MOF-PU nanocomposite in different MB concentrations.

$$A\%=\frac{(A_0-A_t)}{A_0}\times 100 \qquad (1)$$

Based on the results, the increase in MOF amount was resulted in the increase of methylene blue adsorption due to the increase in surface area. These results are based on the report of MB adsorption by Ni-metal organic framework [39] and sulfonated chitosan montmorillonite composite [80]. The methylene blue adsorption was evaluated in different methylene blue concentrations including 2, 3, 4, and 5 mg/L by 0.5 g MOF (Fig. 6 a) and different percentages of nanocomposite including 5 and 10 % at different times (Fig. 6 b). The increase in methylene blue concentration resulted in to increase in adsorption by MOF. The adsorption of MOF-PU nanocomposite was examined at a constant concentration of 4 mg/L for methylene blue solution. According to the nanocomposite result, the increase in MOF percentage was resulted in to increase of methylene blue adsorption due to an increase in surface area. It can be concluded that the obtained nanocomposite provides a large surface area for the adsorption process. Due to its small size and increased surface area and porosity, applications are expanding in various fields [69, 78].

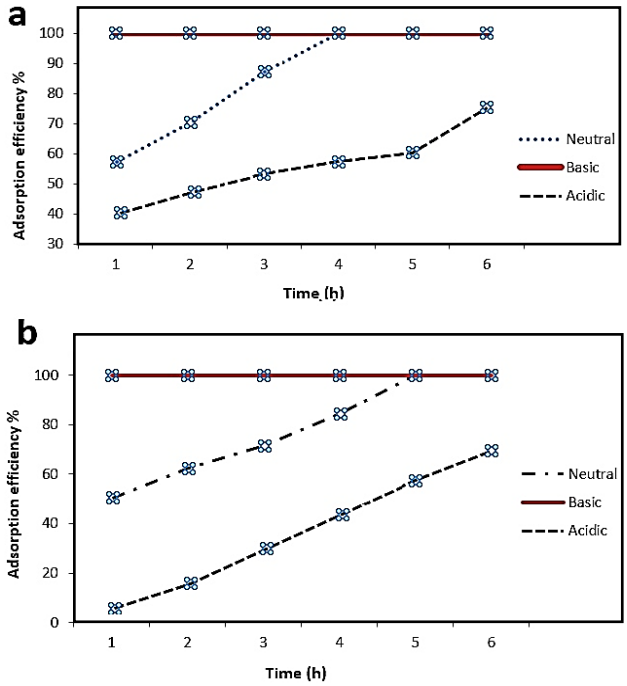

Fig. 7: ***The diagram of MB adsorption by a) MOF and b) MOF-PU nanocomposite in different pH.***

The pH of the methylene blue initial solution was 8.6. By changing the pH of the solutions, positive or negative charges are created on the surface of the environment [62]. The adsorption was studied in different pH of the solution including acidic (pH=4), neutral (pH=7), and basic (pH=9) for 0.5 g MOF with 4 mg/L of methylene blue concentration and 10% nanocomposite with 4 mg/L of methylene blue concentration (Fig. 7). According to the results, higher pH caused more active sites and reduced competition between positive charges and increased methylene blue adsorption through electrostatic gravity. Thus, high numbers of OH^- will be available on the surface. Therefore, the adsorbent surface tends to have

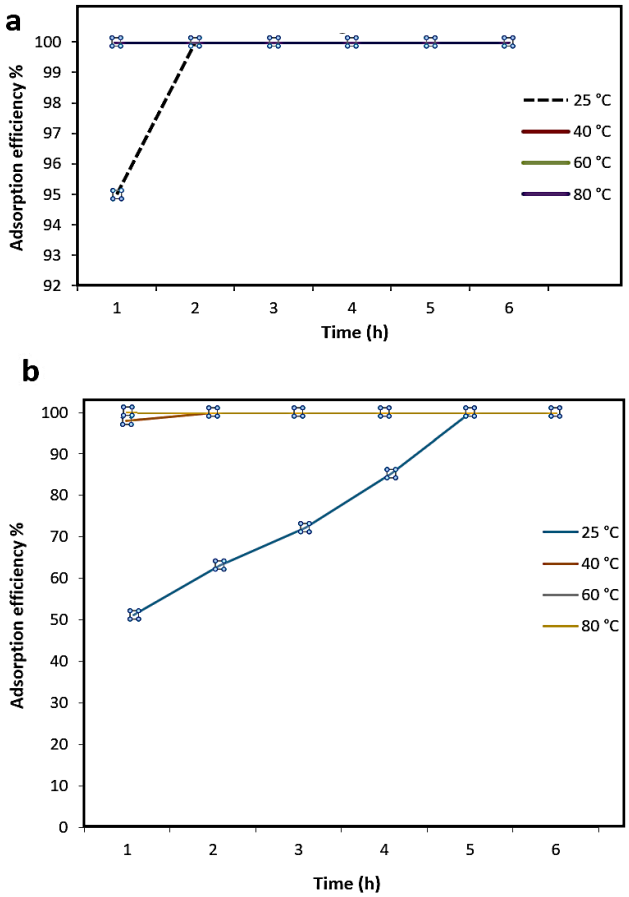

Fig. 8: The diagram of MB adsorption by a) MOF and b) MOF-PU nanocomposite in different temperatures (40, 60 and 80 °C percent adsorption are for MOF and the graphs are stacked. 60 and 80 °C percent adsorption is for MOF-PU nanocomposite and the graphs are stacked).

a negative charge and thus increases the affinity for the exchange of OH^- ions with the cationic solution [81]. In general, changes in the pH of the solution caused various interactions such as attraction or electrostatic repulsion, and hydrogen bond interaction that affect the adsorption efficiency [82]. Methylene blue is a cationic dye. At low pH, the H^+ concentration is high; therefore, the MOF surface charge is positive, which in turn reduces the adsorption of methylene blue. By increasing pH, OH^- concentration gradually increased and methylene blue adsorption on MOF increased [83].

Methylene blue adsorption was evaluated in various temperatures including 25 (ambient), 40, 60, and 80 °C For 0.5 g MOF with 4 mg/L of methylene blue concentration and 10% nanocomposite with 4 mg/L of methylene blue concentration (Fig. 8). The adsorption percentage of MB is 95% (25 °C) and 100% (40, 60, and

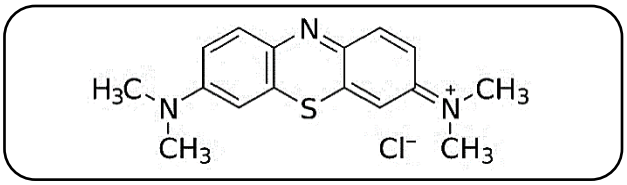

Scheme 1: Structure of MB

80 °C) for MOF and 50% (25 °C), 98% (40 °C), and 100% (60 and 80 °C) for its nanocomposite in 1 h. The increase in temperature was resulted to increase of methylene blue adsorption because of kinetic energy and Brownian motion. Based on the previous report, temperature is directly related to the potential for adsorption by sorbent [63]. Obviously, temperature significantly increases the absorption of MB. By increasing temperature, the adsorption capacity increases, indicating that adsorption is an endothermic process. Increasing temperatures may cause swelling in the porosity and volume of the adsorbent pores, enabling MB molecules to penetrate rapidly on the surface and inside the adsorbent internal pores [84].

Adsorption mechanism

The Chemical structure of methylene blue ($C_{16}H_{18}N_3SCl$) is shown in Scheme 1. Methylene blue is a heterocyclic aromatic chemical compound with dimethyl amino groups in its structure. The mechanism of MB dye adsorption on the sample surface can be inferred from the analysis of FT-IR results, in which the presence of functional groups on the surface was confirmed [85, 86]. According to a previous report, adsorption performance has an important relationship with pore structures [87]. The adsorption mechanism in aqueous solution is based on MOF and its nanocomposite by coordinating the covalent bonding of N group as negative charge with MB dye as positive charge [29, 30] and electrostatic interactions [87, 88]. It is also based on the functional groups of $Zn_2(BDC)_2(DABCO)$ MOF such as BDC ligand (COO^-) and DABCO ligand (N:) with the compounds of methylene blue cationic dye. Also, π–π stacking and hydrogen bonding sequences of MOF and MB dye help to absorb dye [29, 30]. Another interaction could involve hydrogen bonding between the donor and receptor groups of the MOF-MB system [89]. Hence methylene blue as one of the most common members of cationic dyes can be a good choice for adsorption by MOF. Kinetics and removal mechanisms have been reported for methyl orange as an acidic anionic dye [90].

CONCLUSIONS

In this research, $Zn_2(BDC)_2(DABCO)$ MOF adsorbent was synthesized by solvothermal method at 90 °C for 3 h via the self-assembly metal centers and linkers using DMF solvent. Its structural properties were characterized by FT-IR, XRD, FESEM, and BET. Such a synthesized adsorbent has a good surface area (762 m^2/g). Based on the results, the MOF and the MOF-PU nanocomposite were proposed as good candidates for methylene blue adsorption. The effect of different parameters including MOF amount, MB concentrations, pH, and temperature was shown on methylene blue adsorption by MOF and its PU nanocomposite. The potential of this method is that the dye is adsorbed by the sorbent and nano sorbents can be removed from the environment. Therefore, the strength can be a convenient and cost-effective method due to due to its easy and low-cost fabrication, large surface area, and low material consumption. The results showed that MOF and its PU nanocomposite can be an economical source of methylene blue sorbent from an aqueous solution for the development of environmental applications. But the limitation is probably its production on an industrial scale. Also, this method is safe and has no potential risks, so it can have good potential. Future vision can be developed using this nanocomposite.

Acknowledgments

We would like to thank Dr. Mohsen Shahrousvand for providing the polyurethane polymer.

Received: Sep. 11, 2021 ; Accepted: Jan. 3, 2022

References

[1] Yagub M.T., Sen T.K., Afroze S., Ang H.M., Dye and Its Removal from Aqueous Solution by Adsorption: A Review, *Adv Colloid Interface Sci*., **209:** 172-184 (2014).

[2] Rafatullah M., Sulaiman O., Hashim R., Ahmad A., Adsorption of Methylene Blue on Low-Cost Adsorbents: A Review, *J. Hazard. Mater*., **177(1-3):** 70-80 (2010).

[3] Silva F., Nascimento L., Brito M., da Silva K., Paschoal Jr W., Fujiyama R., Biosorption of Methylene Blue Dye Using Natural Biosorbents Made from Weeds, *Materials*., **12(15):** 2486 (2019).

[4] Raeisi Kheirabadi N., Salman Tabrizi N., Sangpour P., Synthesis of Sodium Alginate-Derived Carbon Aerogel for Adsorptive Removal of Methylene Blue, *Iran. J. Chem. Chem. Eng. (IJCCE)*, **39(5):** 157-168 (2020).

[5] Pai S., Kini M.S., Selvaraj R., A Review on Adsorptive Removal of Dyes from Wastewater by Hydroxyapatite Nanocomposites, *ESPR.*, **28:** 11835–11849 (2021).

[6] Crini G., non-Conventional Low-Cost Adsorbents for Dye Removal: A Review, *Bioresour. Technol*., **97(9):** 1061-1085 (2006).

[7] Anastopoulos I., Hosseini-Bandegharaei A., Fu J., Mitropoulos A.C., Kyzas G.Z., Use of Nanoparticles for Dye Adsorption: Review, *J. Disper. Sci. Technol*., **39(6):** 836-847 (2018).

[8] Ajibola Adeyemo A., Olatunbosun Adeoye I., Solomon Bello O., Metal Organic Frameworks as Adsorbents for Dye Adsorption: Overview, Prospects and Future Challenges, *Toxicol. Environ. Chem*., **94(10):** 1846-1863 (2012).

[9] Moradi P., Qanavati R., Mirzaei Ghaleh Ghobadi M., Reducing Nitrate from Water using Lanthanum-Modified Adsorbent: Optimization, Thermodynamics, Kinetics, Isotherms, *Iran. J. Chem. Chem. Eng. (IJCCE)*, **41(5):** 1619-1633 (2022).

[10] Almezgagi M., Guzel Kaya G., Kar Y., Deveci H., Biochar Produced from Co-Pyrolysis of Olive Pomace & Crude Oil as an Adsorbent for Cr (VI) Removal from Aqueous Solutions, *Iran. J. Chem. Chem. Eng. (IJCCE)*, **41(4):** 1199-1210 (2022).

[11] Thusabantu N., Archford Munzeiwa W., Mudavanhu, N., Mukaratirwa-Muchanyereyi N., Chaukura N., Engineered Algal Biochar for the Sequestration of Cu^{2+} from Aqueous Solution, *Iran. J. Chem. Chem. Eng. (IJCCE)*, **41(4):** 1211-1223 (2022).

[12] Dizaj Khalili A., Ghaemi A., Yousefi M., Characterization of Phosphorus and Ground Granulated Blast-Furnace Slags as Low-Cost Adsorbents for Cu(II) Removal; Kinetic, Isotherm, and Thermodynamic Studies, *Iran. J. Chem. Chem. Eng. (IJCCE)*, **41(4):** 1126-1136 (2022).

[13] Mapombere G., Nyoni B., Sibali L.L., Chiririwa H., Seodigeng T., Adsorption of Mercury by Pterocarpus Anglolensis: Study on Adsorption Isotherms and Kinetics *Iran. J. Chem. Chem. Eng. (IJCCE)*, **41(1):** 143-153 (2022).

[14] Vijayaraghavan J., Zunaithur Rahman D., Thivya J., Removal of Ni (II) Ions from Wastewater by Raw and Modified Plant Wastes as Adsorbents: A Review, *Iran. J. Chem. Chem. Eng. (IJCCE)*, **41(1):** 174-206 (2022).

[15] Thamilarasi Maria Joseph V., Molagoundampalayam Venkatachalam S., Arun Kumar P., Adsorption of Molybdenum from Wastewater by Surface Altered Agricultural Solid Waste, *Iran. J. Chem. Chem. Eng. (IJCCE)*, **41(6):** 1883-1895 (2022).

[16] Djamila D., Chabani M., Hank Z., Combined Microwave-Peanut Hull Based Activated Carbon Process in the Removal of Oxytetracycline (OXT) from Aqueous Solution, *Iran. J. Chem. Chem. Eng. (IJCCE)*, **41(6):** 1896-1906 (2022).

[17] Pedram, T., Eshaghi, Z., Ahmadpour, A., Nakhaei, A., Optimization of Adsorption Parameters Using Central Composite Design for the Removal of Organosulfur in Diesel Fuel by Bentonite-Supported Nanoscale NiO-WO_3, *Iran. J. Chem. Chem. Eng. (IJCCE)*, **41(3):** 808-820 (2022).

[18] Adeyemo A.A., Adeoye I., Adeoye O.S., Adsorption of Dyes using Different Types of Clay: A Review, *Appl. Water Sci.*, **7:** 543–568 (2017).

[19] Iran Manesh M., Sohrabi Saeid M.R., Nik M., Nanoscale Zero-Valent Iron Supported on Graphene Novel Adsorbent for the Removal of Diazo Direct Red 81 from Aqueous Solution: Isotherm, Kinetics, and Thermodynamic Studies, *Iran. J. Chem. Chem. Eng. (IJCCE)*, **41(6):** 1844-1855 (2022).

[20] Lamari R., Benotmane B., Mostefa F., Removal of Methyl Orange from Aqueous Solution Using Zeolitic Imidazolate Framework-11: Adsorption Isotherms, Kinetics and Error Analysis, *Iran. J. Chem. Chem. Eng. (IJCCE)*, **41(6):** 1985-1999 (2022).

[21] Alkan S., Karakoc E., Caliskan M., Savran A, Kubilay S., Adsorption of Textile Dyes on Willow Tree Pollen: Determination of Equilibrium, Kinetics, and Thermodynamic, *Iran. J. Chem. Chem. Eng. (IJCCE)*, **41(5):** 1588-1601 (2022).

[22] Ratnam Myneni V., Rao Kanidarapu N., Shaik F., Vangalapati M., Response Surface Modeling of the Removal of Methyl Orange Dye from an Aqueous Solution Using Magnesium Oxide Nanoparticles Immobilized on Chitosan, *Iran. J. Chem. Chem. Eng. (IJCCE)*, **41(5):** 1602-1618 (2022).

[23] Davarnejad, R., Azizi, A., Asadi, S., Mohammadi, M., Green Synthesis of Copper Nanoparticles Using Centaurea Cyanus Plant Extract: A Cationic Dye Adsorption Application, *Iran. J. Chem. Chem. Eng. (IJCCE)*, **41(1):** 1-14 (2022).

[24] Belgacem A., Ould Brahim I., Belmedani M., Hadoun H., Removal of Methyl Green Dye from Aqueous Solutions Using Activated Carbon Derived from Cryogenic Crushed Waste Tires, *Iran. J. Chem. Chem. Eng. (IJCCE)*, **41(1):** 207-219 (2022).

[25] Nacer D., Fatima O., Reda M., Synthesis of New Organo-Inorgano-Clay Materials Based on Metal Ions, CTMAB, and Bentonite. Application for Removal of Acid Dye, *Iran. J. Chem. Chem. Eng. (IJCCE)*, **41(1):** 431-445 (2022).

[26] Nazim Younes B., Djame N., Samira A., NaY Zeolite and TiO_2 Impregnated NaY Zeolite for the Adsorption and Photocatalytic Degradation of Methylene Blue under Sunlight, *Iranian Journal Chemistry and Chemical Engineering (IJCCE)*, **41(6):** 1907-1920 (2022).

[27] Cheng T., Chen C., Ye C., Xie W., Zhang Z., Yuan T., Synthesis of $KBiO_3$/Nano-Ag_3PO_4 Composite Photocatalyst and its Application for Degradation of Organic Pollutants under Visible Light, *Iran. J. Chem. Chem. Eng. (IJCCE)*, **41(6):** 1942-1960 (2022).

[28] Liang H., Hu X., Preparation of Magnetic Cellulose Nanocrystal-Modified Diatomite for Removal of Methylene Blue from Aqueous Solutions, *Iran. J. Chem. Chem. Eng. (IJCCE)*, **41(3):** 787-798 (2022).

[29] Motakef-Kazemi N., Zinc Based Metal–Organic Framework for Nickel Adsorption in Water and Wastewater Samples by Ultrasound Assisted-Dispersive-Micro Solid Phase Extraction Coupled to Electrothermal Atomic Absorption Spectrometry, *AMECJ.*, **3(4):** 5-16 (2020).

[30] Motakef-Kazemi N., A Novel Sorbent based on Metal–Organic Framework for Mercury Separation from Human Serum Samples by Ultrasound Assisted-Ionic Liquid-Solid Phase Microextraction, *AMECJ.*, **2:** 67-78 (2019).

[31] Dutta S., Gupta B., Kumar Srivastava S., Kumar Gupta A., Recent Advances on the Removal of Dyes from Wastewater Using Various Adsorbents: A Critical Review. *Mater. Adv.*, **2**: 4497-4531 (2021).

[32] Jawad, A.H., Abdulhameed, A.S., Najwa Abd Malek, N., ALOthman, Z.A., Statistical Optimization and Modeling for Color Removal and COD Reduction of Reactive Blue 19 Dye by Mesoporous Chitosan-Epichlorohydrin/Kaolin Clay Composite, *Int. J. Biol*., **164:** 4218-4230 (2020).

[33] Jawad A.H., Saud Abdulhameed A.S., Kashi E., Mundher Yaseen Z., ALOthman Z.A., Rizwan Khan M., Cross-Linked Chitosan-Glyoxal/Kaolin Clay Composite: Parametric Optimization for Color Removal and COD Reduction of Remazol Brilliant Blue R Dye, *J. Polym. Environ*., **30:** 164-178 (2021).

[34] Shazwani Abdul Mubarak N., Chuan T.W., Khor H.P., Jawad A.H., Wilson L.D., Sabar S., Immobilized Fe-Loaded Chitosan Film for Methyl Orange Dye Removal: Competitive Ions, Reusability, and Mechanism, *J. Polym. Environ*., **29:** 1050–1062 (2021).

[35] Bahrudin N.N., Nawi M.A., Jawad A.H., Sabar S., Adsorption Characteristics and Mechanistic Study of Immobilized Chitosan-Montmorillonite Composite for Methyl Orange Removal, *J. Polym. Environ*., **28:** 1901–1913 (2020).

[36] Zhua Q.L., Xu Q., Metal–Organic Framework Composites, *Chem. Soc. Rev.*, **43:** 5468-5512 (2014).

[37] Li H., Eddaoudi M., O'Keeffe M., Yaghi, O., Design and Synthesis of An Exceptionally Stable and Highly Porous Metal-Organic Framework, *Nature*, **402:** 276-279 (1999).

[38] Motakef-Kazemi N., Rashidian M., Taghizadeh Dabbagh S., Yaqoubi M., Synthesis and Characterization of Bismuth Oxide Nanoparticles by Thermal Decomposition of Bismuth-based MOF and Evaluation of its Nanocomposite, *Iranian Journal Chemistry and Chemical Engineering* (*IJCCE*), **40(1):** 11-19 (2021).

[39] Pettinari C., Marchetti F., Mosca N., Tosi G., Drozdov A., Application of Metal−Organic Frameworks, *Polym. Int*., **66(6):** 731-744 (2017).

[40] Hajiashrafi S., Motakef-Kazemi N., Preparation and Evaluation of ZnO Nanoparticles by Thermal Decomposition of MOF-5, *Heliyon*., **5(9):** e02152 (2019).

[41] Motakef-Kazemi N., Shojaosadati S.A., Morsali A., In Situ Synthesis of a Drug-Loaded MOF at Room Temperature, *Micropor Mesopor Mat*., **186:** 73-79 (2014).

[42] Motakef-Kazemi N., Shojaosadati S.A., Morsali A., Evaluation of the Effect of Nanoporous Nanorods $Zn_2(bdc)_2(dabco)$ Dimension on Ibuprofen Loading and Release, *J. Iran. Chem. Soc*., **13(7):** 1205-1212 (2016).

[43] Yaghi O.M., Li H., Hydrothermal Synthesis of a Metal-Organic Framework Containing Large Rectangular Channels, *J. Am. Chem. Soc*., **117(41):** 10401–10402 (1995).

[44] Klinowski J., Almeida Paz F.A., Silva P., Rocha J., Microwave-Assisted Synthesis of Metal–Organic Frameworks, *Dalton Trans*., **40:** 321-330 (2011).

[45] Son W.J., Kim J., Kim J., Ahn W.S., Sonochemical Synthesis of MOF-5. *Chem. Commun*., **47:** 6336-6338 (2008).

[46] Al-Kutubi H., Gascon J., Sudhölter E.J.R., Rassaei L., Electrosynthesis of Metal–Organic Frameworks: Challenges and Opportunities, *Chem. Electro. Chem*., **2(4):** 462-474(2015).

[47] Wang Z., Li Z., Nga M., Milner P.J., Rapid Mechanochemical Synthesis of Metal–Organic Frameworks using Exogenous Organic Base, *Dalton Trans*., **49:** 16238-16244 (2020).

[48] Ataei F., Dorranian D., Motakef-Kazemi N., Bismuth-based Metal–Organic Framework Prepared by Pulsed Laser Ablation Method in Liquid, *JTAP*., **14:** 1-8 (2020).

[49] Ataei F., Dorranian D., Motakef-Kazemi N., Synthesis of MOF-5 Nanostructures by Laser Ablation Method in Liquid and Evaluation of its Properties, *J. Mater. Sci.: Mater. Electron*., **32:** 3819-3833 (2021).

[50] Jamal Uddin M., Ampiaw R.E., Lee W., Adsorptive Removal of Dyes from Wastewater using a Metal-Organic Framework: A Review, *Chemosphere*., **284:** 131314 (2021).

[51] Mehmandoust M.R., Motakef-Kazemi N., Ashouri F., Nitrate Adsorption from Aqueous Solution by Metal–Organic Framework MOF-5, *Iran. J. Sci.. Technol. A*., **43(2):** 443-449 (2019).

[52] Dehghan A., Mohammadi A.A, Yousefi M., Najafpoor A.A., Shams M., Rezania S., Enhanced Kinetic Removal of Ciprofloxacin onto Metal-Organic Frameworks by Sonication, Process Optimization and Metal Leaching Study, *Nanomaterials*., **9:** 1422 (2019).

[53] Saghia M.H., Chabot B., Rezania S., Sillanpää M., Mohammadi A.A., Shams M., Alahabadi A., Water-Stable Zirconium and Iron-Based Metal-Organic Frameworks (MOFs) as Fluoride Scavengers in Aqueous Medium, *Sep. Purif. Technol*., **279:** 118645 (2021).

[54] Lin S., Song Z., Che G., Ren A., Li P., Liu C., Zhang J., Adsorption Behavior of Metal–Organic Frameworks for Methylene Blue from Aqueous Solution, *Micropor Mesopor Mat*., **193:** 27-34 (2014).

[55] Zhao X., Liu S., Tang Z., Niu H., Cai Y., Meng W., Wu F., Giesy J.P., Synthesis of Magnetic Metal-Organic Framework (MOF) for Efficient Removal of Organic Dyes from Water, *Sci Rep*., **5:** 11849 (2015).

[56] Haque E., Won Jun J., Hwa Jhung S., Adsorptive Removal of Methyl Orange and Methylene Blue from Aqueous Solution with a Metal-Organic Framework Material, Iron Terephthalate (MOF-235), *J. Hazard. Mater*., **185:** 507-511 (2011).

[57] Huda Paiman S., Rahman M.A., Uchikoshi T., Abdullah N., Dzarfan Othman M.H., Jaafar J., Hamimah Abas K., Fauzi Ismail A., Functionalization Effect of Fe-Type MOF for Methylene Blue Adsorption, *J. Saudi Chem. Soc*., **24(11):** 896-905 (2020).

[58] Arora C., Soni S., Sahu S., Mittal J., Kumar P., Bajpai P.K., Iron Based Metal Organic Framework for Efficient Removal of Methylene Blue Dye from Industrial Waste, *J. Mol. Liq*., **284:** 343-352 (2019).

[59] Shi L., Hu L., Zheng J., Zhang M., Xu J., Adsorptive Removal of Methylene Blue from Aqueous Solution using a Ni-metal Organic Framework Material, *J. Disper. Sci. Technol*., **37:** 1226-1231 (2016).

[60] Yang Q., Wiersum A.D., Llewellyn P.L., Guillerm V., Serred C., Maurin G., Functionalizing Porous Zirconium Terephthalate UiO-66(Zr) for Natural Gas Upgrading: A Computational Exploration, *Chem. Commun.*, **47:** 9603-9605 (2011).

[61] Saghanejhad Tehrani M., Zare-Dorabei R., Highly Efficient Simultaneous Ultrasonic-Assisted Adsorption of Methylene Blue and Rhodamine B onto Metal Organic Framework MIL-68(Al): Central Composite Design Optimization, *RSC Adv.*, **6:** 27416-27425 (2016).

[62] Yanga Q., Rena S.S., Zhaoa Q., Lua R., Hang C., Chena Z., Zheng H., Selective Separation of Methyl Orange from Water using Magnetic ZIF-67 Composites, *Chem. Eng. J*., **333:** 49-57 (2018).

[63] Odar M., Motakef Kazemi N., Nanohydroxyapatite and its Polycaprolactone Nanocomposite for Lead Sorbent from Aqueous Solution, *Nanomed. Res. J*., **5:** 143-151 (2020).

[64] Sharma R.K., Solanki K., Dixit R., Sharma S., Dutta S., Nanoengineered Iron Oxide-based Sorbents for Separation of Various Water Pollutants: Current Status, Opportunities and Future Outlook, *Environ. Sci.: Water Res. Technol*., **7:** 818-860 (2021).

[65] Al-Gorair A.S., Treatment of Wastewater from Cationic Dye using Eco-Friendly Nanocomposite: Characterization, Adsorption and Kinetic Studies, *Egypt J. Aquat. Res*., **45(1):** 25-31 (2019).

[66] Moradi O., Sharma G., Emerging Novel Polymeric Adsorbents for Removing Dyes from Wastewater: A Comprehensive Review and Comparison with other Adsorbents, *Environ. Res*., **201:** 111534 (2021).

[67] Gouthaman A., Auslin Asira J., Gnanaprakasam A., Sivakumar V.M., Thirumarimurugan M., Riswan Ahamed M.A., Azarudeen R.S., Enhanced Dye Removal using Polymeric Nanocomposite through Incorporation of Ag Doped ZnO Nanoparticles: Synthesis and Characterization, *J. Hazard. Mater*., **373:** 493-503 (2019).

[68] Robaina N.F., Soriano S., Cassella R.J., Polyurethane Foam Loaded with SDS for the Adsorption of Cationic Dyes from Aqueous Medium: Multivariate Optimization of the Loading Process, *J. Hazard. Mater*., **167(1-3):** 653-659 (2009).

[69] Motakef-Kazemi N., Odar M., Adsorption and Determination of Lead in Water and Human Urine Samples based on $Zn_2(BDC)_2(DABCO)$ MOF as Polycaprolactone Nanocomposite by Suspension Micro Solid Phase Extraction Coupled to UV–VIS Spectroscopy. *AMECJ*., **4(3):** 5-20 (2021).

[70] Reghioua A., Barkat D., Jawad A.H., Abdulhameed A.S., Rizwan Khan M., Synthesis of Schiff's base Magnetic Crosslinked Chitosan-Glyoxal/ZnO/Fe_3O_4 Nanoparticles for Enhanced Adsorption of Organic Dye: Modeling and Mechanism Study, *Sustain. Chem. Pharm*., **20:** 100379 (2021).

[71] Reghioua A., Barkat D., Jawad A.H., Saud Abdulhameed S., Al-Kahtani A.A., ALOthman Z.A., Parametric Optimization by Box–Behnken Design for Synthesis of Magnetic Chitosan-Benzil/ZnO/Fe_3O_4 Nanocomposite and Textile Dye Removal, *J. Environ. Chem. Eng*., **9(3):** 105166 (2021).

[72] Jawad A.H., Awad Mohammed I., Saud Abdulhameed A., Tuning of Fly Ash Loading into Chitosan-Ethylene Glycol Diglycidyl ether Composite for Enhanced Removal of Reactive red 120 Dye: Optimization using the Box–Behnken Design, *J Polym Environ*., **28:** 2720–2733 (2020).

[73] Jawad A.H., Solehah Ahmad Norrahma S., Hamee, B.H., Ismail K., Chitosan-Glyoxal Film as a Superior Adsorbent for Two Structurally Different Reactive and Acid Dyes: Adsorption and Mechanism Study, *Int. J. Biol*., **135:** 569-581 (2019).

[74] Marahel F., Mombeni Goodajdar B., Niknam L., Faridnia M., Pournamdari E., Doost S.M., Ultrasonic Assisted Adsorption of Methylene Blue Dye and Neural Network Model for Adsorption of Methylene Blue Dye by Synthesised Mn-doped PbS Nanoparticles, *Int. J. Environ. Anal. Chem.*, **89:** 1-22 (2021).

[75] Bhattacharjee C., Dutta S., Saxena V.K., A Review on Biosorptive Removal of Dyes and Heavy Metals from Wastewater using Watermelon Rind as Biosorbent, *Environ. Adv*., **2:** 100007 (2020).

[76] Coeli Moreira Dias R., Miranda Góes A., Serakides R., Ayres E., Lambert Oréfice R., Porous Biodegradable Polyurethane Nanocomposites: Preparation, Characterization, and Biocompatibility Tests, *Mater. Res*., **13(2):** 211-218 (2010).

[77] Jawad A.H., Sabar S., Azlan Mohd Ishak M., Wilson L.D., Solehah Ahmad Norrahma S., Talari M.K., Farhan A.M., Microwave-Assisted Preparation of Mesoporous Activated Carbon from Coconut (Cocos Nucifera) Leaf by H_3PO_4-Activation for Methylene Blue Adsorption, *Chem. Eng. Commun*., **204(10):** 1563-5201 (2017).

[78] Haftan F., Motakef Kazemi N., The Sorbent based on MOF-5 and its Polyurethane Nanocomposite for Copper Adsorption from Aqueous Solution, *Nanomed. Res. J*., **6(3):** 1-9 (2021).

[79] Sing K.S.W., Reporting Physisorption Data for Gas/Solid Systems with Special Reference to the Determination of Surface Area and Porosity, *Pure Appl. Chem*., **54(11):** 2201-2218 (1982).

[80] Shazwani Abdul Mubarak N., Bahrudin N.N., Jawad A.H., Hameed B.H., Sabar S., Microwave Enhanced Synthesis of Sulfonated Chitosan-Montmorillonite for Effective Removal of Methylene Blue, *J. Polym. Environ*., **29:** 4027–4039 (2021).

[81] Faraji H., Mohamadi A.A., Soheil Arezomand H.R., Mahvi A.H., Kinetics and Equilibrium Studies of the Removal of Blue Basic 41 and Methylene Blue from Aqueous Solution Using Rice Stems, *Iranian Journal Chemistry and Chemical Engineering (IJCCE).*, **34(3):** 33-42 (2015).

[82] Li C., Xiong Z., Zhang J., Wu C., The Strengthening Role of the Amino Group in Metal−Organic Framework MIL-53 (Al) for Methylene Blue and Malachite Green Dye Adsorption, *J. Chem. Eng. Data*., **60(11):** 3414–3422 (2015).

[83] Mohammadi A.A., Alinejad A., Kamarehie B., Javan S., Ghaderpoury A., Ahmadpour M., Ghaderpoori M., Metal-Organic Framework Uio-66 for Adsorption of Methylene Blue dye from Aqueous Solutions, *Int. J. Environ. Sci. Techno*., **14:** 1959–1968 (2017).

[84] Fallah Shojaei A., Tabatabaeian K., Zebardast M., Ferric Ion Modified Nano-MOF-5 Synthesized by a Direct Mixing Approach: A Highly Efficient Adsorbent for Methylene Blue Dye, *Scientia Iranica*., **25(3):** 1323-1334 (2018).

[85] Jawad A.H., Bardhan M., Islam A., Islam A., Syed-Hassan S.S.A., Surip S.N., Insights into the Modeling, Characterization and Adsorption Performance of Mesoporous Activated Carbon from Corn Cob Residue via Microwave-Assisted H_3PO_4 Activation, *Surf*. **21:** 100688 (2020).

[86] Jawad A.H., Nadiah Mohd Firdaus Hum N., Saud Abdulhameed A., Azlan Mohd Ishak M., Mesoporous Activated Carbon from Grass Waste via H_3PO_4-Activation for Methylene Blue Dye Removal: Modelling, Optimization, and Mechanism Study, *International Journal of Environmental Analytical Chemistry*., **17:** 102 (2020).

[87] Li X., Han D., Zhang M., Li B., Wang Z., Gong Z., Liu P., Zhang Y., Yang X., Removal of Toxic Dyes from Aqueous Solution using New Activated Carbon Materials Developed from Oil Sludge Waste, *Colloid., Surf. A-Physicochem. Eng. Asp.*, **578:** 123505 (2019).

[88] Jawad A.H., Abdulhameed A.S., Wilson L.D., Syed-Hassan S.S.A., ALOthman Z.A., Rizwan Khan M., High Surface Area and Mesoporous Activated Carbon from KOH-Activated Dragon Fruit Peels for Methylene Blue Dye Adsorption: Optimization and Mechanism Study, *Chin. J. Chem. Eng*., **32:** 281-290 (2021).

[89] Jawad A.H., Saud Abdulhameed A., Hanafiah M.A.K.M., ALOthman Z.A., Rizwan Khan M., Surip S.N., Numerical Desirability Function for Adsorption of Methylene Blue Dye by Sulfonated Pomegranate Peel Biochar: Modeling, Kinetic, Isotherm, Thermodynamic, and Mechanism Study, *Korean J. Chem. Eng*., **38(7):** 1499-1509 (2021).

[90] Ghourchian F., Motakef-Kazemi N., Ghasemi E., Ziyadid H., Zn-based MOF-Chitosan-Fe_3O_4 Nanocomposite as an Effective Nano-Catalyst for Azo Dye Degradation, *J. Environ. Chem. Eng*., **9(6):** 106388 (2021).